

# Fast TeV variability from misaligned minijets in the jet of M87

Dimitrios Giannios<sup>1\*</sup>, Dmitri A. Uzdensky<sup>1</sup> and Mitchell C. Begelman<sup>2,3</sup>

<sup>1</sup>*Department of Astrophysical Sciences, Peyton Hall, Princeton University, Princeton, NJ 08544, USA*

<sup>2</sup>*Joint Institute for Laboratory Astrophysics, University of Colorado, Boulder, CO 80309, USA*

<sup>3</sup>*Department of Astrophysical and Planetary Sciences, University of Colorado, Boulder*

Received / Accepted

## ABSTRACT

The jet of the radio galaxy M87 is misaligned, resulting in a Doppler factor  $\delta \sim 1$  for emission of plasma moving parallel to the jet. This makes the observed fast TeV flares on timescales of  $t_v \sim 5R_g/c$  harder to understand as emission from the jet. In previous work, we have proposed a jets-in-a-jet model for the ultra-fast TeV flares with  $t_v \ll R_g/c$  seen in Mrk 501 and PKS 2155-304. Here, we show that about half of the minijets beam their emission outside the jet cone. Minijets emitting off the jet axis result in rapidly evolving TeV (and maybe lower energy) flares that can be observed in nearby radio galaxies. The TeV flaring from M87 fits well into this picture, if M87 is a misaligned blazar.

**Key words:** galaxies: active – galaxies: individual: M87 – galaxies: jets – radiation mechanisms: non-thermal – gamma rays: theory

## 1 INTRODUCTION

The jet originating from the nucleus of M87 has been well studied at all wavelengths thanks to its proximity. Its radio images and modeling of its interaction with its environment suggest that the jet is misaligned by  $\theta \sim 30^\circ$  with respect to our line of sight (Biretta, Zhou & Owen 1995; Bicknell & Begelman 1996).

Recently several groups (Aharonian et al. 2006; Albert et al. 2008; Acciari et al. 2008) have reported TeV emission from M87 that shows rapid variability on timescales of  $\sim 1$  day. The fast flaring implies emitting regions of typical length scale of  $l_{em} \lesssim 5 \times R_g \delta$ , where  $R_g = GM/c^2$  and  $M = 3 \times 10^9 M_\odot$  is the mass of the black hole measured by gas dynamics in the vicinity of the black hole (Macchetto et al. 1997)<sup>1</sup> and  $\delta$  is the Doppler factor of the emitting material. Since the jet from M87 is misaligned by  $\sim 30^\circ$ , any Doppler factor associated with the bulk motion of the jet is  $\delta \sim 1$ , leading to  $l_{em} \lesssim 5R_g$ .

Aharonian et al. (2006) proposed that the TeV emitting region is not associated with the jet but with the magnetosphere of the black hole (Levinson 2000). Alternatively, the TeV emission may originate in the sub-pc jet while the jet is collimating (Lenain et al. 2008) or in (at least) two zone models such as a jet with a fast spine and a slower layer (Tavecchio & Ghisellini 2008) or a decelerating jet (Georganopoulos, Perlman & Kazanas 2005). The knot HST-1

has also been discussed as a possible source of the TeV emission (Cheung, Harris & Stawarz 2007).

The latest (February 2008) observed TeV flaring of M87 was caught simultaneously in radio VLBI and X-rays (Acciari et al. 2009). At the period of the TeV activity, the radio started to show a gradual rise that continued over the succeeding months. The VLBI map showed new radio blobs starting to move outward from within  $\sim 100R_g$  from the black hole, suggesting that the gamma-ray flare comes from very close to the black hole. While the X-rays from the nucleus were climbing during the flare, HST-1 was in a low X-ray state, making it unlikely that HST-1 is the source of the flares.

Fast flaring on timescales  $t_v \sim R_g/c$  observed in blazars is attributed to large Doppler factors  $\delta \gg 1$  of emitting plasma associated with relativistic jets pointing directly at us. The very fast TeV variability of the blazars Mrk 501 and PKS 2155-304 (Aharonian et al. 2007; Albert et al. 2007) corresponds to  $t_v \sim 0.1R_g/c$  and poses strong constraints to any model. For the TeV radiation to avoid absorption at the source, the emitting material must move with a bulk Lorentz factor  $\Gamma_{em} \gtrsim 50$  (Begelman, Fabian & Rees 2008) while resolved patterns on sub-pc scales are compatible with moderate Lorentz factors  $\Gamma_j < 10$  for the jet (Piner & Edwards 2004; Giroletti et al. 2004). In a previous work, we proposed that very rapid TeV variability observed in blazars comes from blobs of energetic particles that are moving with relativistic speed *relative to* the mean flow of the jet (Giannios, Uzdensky & Begelman 2009). We associate these minijets with the material outflowing from reconnection events in a Poynting-flux dominated jet. Jets with typical  $\Gamma_j \lesssim 10$  (as indicated by proper motions) would thus contain minijets that move with  $\Gamma_{em} \sim 100 \gg \Gamma_j$  relative to the observer, as needed for TeV radiation to escape the source and power flares with  $t_v \ll R_g/c$ .

A natural consequence of the jets-in-a-jet model is that, while

\* E-mail: giannios@astro.princeton.edu (DG)

<sup>1</sup> Gebhardt & Thomas (2009) claim that the black hole mass is a factor of 2 larger than previously thought. While in this paper, we keep  $M = 3 \times 10^9 M_\odot$  as the reference value for the black hole mass in M87, a larger black hole corresponds to more extreme variability of the TeV emission that strengthens our main arguments.

the emission of about half of the minijets is beamed at an angle  $\theta \lesssim 1/\Gamma_j$  with respect to the jet axis, the rest emit outside the emission cone of the jet. In this paper, we explore the emission from these “misaligned” minijets. We show that the probability that a minijet is *observed* to emit at an angle  $\theta$  depends rather weakly on  $\theta$ . We calculate the energetics and timescales of emission from minijets pointing off the jet axis. Off-axis minijets are bright enough to be observed in nearby radio galaxies. Finally, we apply the jets-in-a-jet model to the fast TeV flaring observed in M87.

## 2 JETS IN A JET

Our main idea of “jets-in-a-jet” is that dissipation of magnetic energy in the jet (e.g., the result of jet instabilities) leads to minijets of energetic particles that move relativistically *within* the jet. Emission from the minijet results in the observed short-timescale flaring. Depending on the direction of motion of the minijet (in the jet rest frame), a minijet emits within the cone of the jet or outside it. In jets moving toward our line of sight (blazars), emission from minijets results in powerful, rapidly evolving flares while in misaligned jets (e.g., in radio galaxies), minijets lead to weaker but still rather rapid flares.

We believe that jets-in-a-jet may be expected in a Poynting-flux dominated flow. They can form in reconnecting regions of strongly magnetized plasma. The magnetic reconnection may result from the nonlinear evolution of kink instabilities in the jet (Eichler 1993; Begelman 1998; Appl, Lery & Baty 2000; Giannios & Spruit 2006; Moll, Spruit & Obergaulinger 2008; Moll 2009; but see McKinney & Blandford 2009) or reversals of the magnetic field polarity in the inner disk/black hole magnetosphere (Giannios et al. 2009). Interestingly, recent evidence for such reversals come from the observed “flip” in the gradient of the Faraday rotation across the jet of B1803+784 between the 2000 and 2002 observations of the source (Mahmud, Gabuzda & Bezrukovs 2009). A similar scenario of relativistic motions within the jet has also been explored in the context of gamma-ray bursts (GRBs). Minijets (caused by relativistic turbulence or magnetic reconnection) may be responsible for the observed variability of the GRB emission (Blandford 2002; Lyutikov 2006a,b; Narayan & Kumar 2008; Lazar, Nakar & Piran 2009).

Consider a jet that moves radially with bulk  $\Gamma_j$ , in which a minijet develops with a Lorentz factor  $\Gamma_{co}$  at an angle  $\theta'$  with respect to the radial direction (both measured in the jet rest frame). All primed/tilded quantities are measured in the rest frame of the jet/minijet respectively. In the lab frame the minijet moves with

$$\Gamma_{em} = \Gamma_j \Gamma_{co} (1 + v_j v_{co} \cos \theta') \quad (1)$$

and at an angle

$$\tan \theta = \frac{v_{co} \sin \theta'}{\Gamma_j (v_{co} \cos \theta' + v_j)} \quad (2)$$

with respect to the radial direction. For  $\theta' \sim \pi/2$  and  $v_{co}, v_j \simeq 1$ , expressions (1) and (2) give  $\Gamma_{em} \sim \Gamma_j \Gamma_{co}$  and  $\theta \sim 1/\Gamma_j$ . Minijets moving at  $\theta > 1/\Gamma_j$  have more moderate bulk Lorentz factor in the lab frame but, in many cases, larger than that of the bulk of the jet  $\Gamma_j$  (see next section).

From eq. (2), one can immediately see that for  $\theta' < \pi/2$  the emission takes place at  $\theta < 1/\Gamma_j$ , i.e., within the emission cone of the jet and vice versa. In the magnetic reconnection picture, every dissipation event results in a pair of mini jets that leave the reconnection region at opposite directions  $\theta'$  and  $\pi - \theta'$ . *Since the*

*distribution of  $\theta'$  of the minijets is symmetric around  $\theta' = \pi/2$ , for every minijet that is beamed within the jet  $1/\Gamma_j$  emission cone there is another minijet that points outside.*

### 2.1 Distribution of emitting angles of minijets with respect to the jet axis

In this section, we explore how the angular dependence of the emission from the minijets is connected to their assumed distribution of directions in the jet rest frame. We find that the probability that the observer is located within the emission cone of a minijet is rather insensitive to the inclination of the jet with respect to the observer.

We consider a relativistic conical jet with opening angle  $\theta_j \sim 1/\Gamma_j$ . Emission associated with the bulk motion of the jet is beamed at the observer when the latter is located at an angle  $\theta \lesssim 1/\Gamma_j$  with respect to the jet axis. An “off-axis observer” is one for which  $\theta > 1/\Gamma_j$ . We measure how “off-axis” the observer is located by the parameter  $\alpha$  defined as:

$$\theta \equiv \frac{\alpha}{\Gamma_j}. \quad (3)$$

If an observer is located at an angle  $\theta$  with respect to the jet axis, how likely is it that the emission from a minijet takes place within the observer’s cone? As discussed above, in the lab frame, the majority of minijets point at small angle  $\theta$  or corresponding  $\alpha \lesssim$  a few. On the other hand, minijets pointing more off-axis have lower bulk Lorentz factors and therefore, wider beaming angles as we will see. The net result is that there is almost uniform probability that a minijet is observed at any angle  $\theta$ .

To quantify this statement, we consider several different cases for the distribution  $P(\Omega')d\Omega'$  of the angle  $\theta'$  of the minijets in the jet rest frame. We consider distributions that are symmetric around  $\theta' = \pi/2$ , as expected from the formation of pairs of counter-streaming minijets that result from magnetic reconnection. We consider 3 cases:  $P(\Omega') \propto \sin^n \theta'$ , for  $n = 0, 1, 2$ . The  $n = 0$  case corresponds to the isotropic distribution. For  $n = 1, 2$  the distributions increasingly peak around  $\theta' = \pi/2$ . We think it is very plausible that the reconnecting current sheets are preferentially oriented perpendicular to the jet direction (e.g., a sequence of toroidal fields with reversing radial currents) leading to the ejection of minijets preferably at  $\theta' \sim \pi/2$ .

We assemble a large number of minijets with  $\theta'$  drawn from the above distributions and calculate the distribution  $P(\alpha)d(\alpha)$  of emission angle  $\alpha$  using the expression (2). For the results shown in Fig. 1, we have set  $\Gamma_j = \Gamma_{co} = 10$ . Very similar angular distributions are found for other values of  $\Gamma_j, \Gamma_{co} \gg 1$ . The distribution of direction of the minijets peaks at  $\alpha \sim 1$  (i.e., at angle  $\theta \sim 1/\Gamma_j$ ). For increasing  $n$ , the  $0.5 \lesssim \alpha \lesssim 2$  angles become more likely. This is expected since the number of minijets moving at  $\theta' \sim \pi/2$  (which results in  $\alpha \sim 1$ ) increases with  $n$ . Furthermore, by definition of the symmetry of the distribution around  $\theta' = \pi/2$ , about half of the jets point at  $\alpha > 1$ , independently of  $n$ .

To calculate the probability distribution that a blob is *observed* at an angle  $\theta \equiv \alpha/\Gamma_j$  one has to take into account that the emission of a blob is beamed into a narrow cone of  $\Omega_{em} \propto 1/\Gamma_{em}^2$ . In Fig. 2, we show the distribution  $P(\alpha)d\Omega/\Gamma_{em}^2$  which we refer as the “observed angular distribution”  $P_{obs}(\alpha)d\Omega$  of the minijets.

From Fig. 2, it is clear that for  $n = 0$  the observed angular distribution of the minijets is almost isotropic. For  $n = 1, 2$  it slightly favors  $0.5 \lesssim \alpha \lesssim 3$ . The reason for  $P_{obs}$  being much flatter than  $P$  is that, although most minijets (per unit of solid angle) point within the jet cone, their emission is beamed within a very narrow cone.

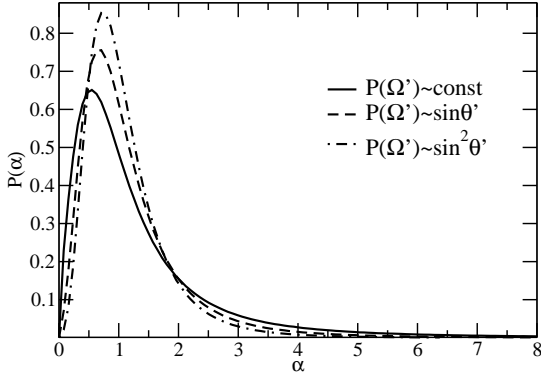


**Figure 1.** Distribution  $P(\alpha)d\alpha$  of direction of minijets in the lab frame (where  $\alpha = \theta\Gamma_j$ ) for different distributions  $P(\Omega')d\Omega'$  of direction of the minijets (in the jet rest frame).

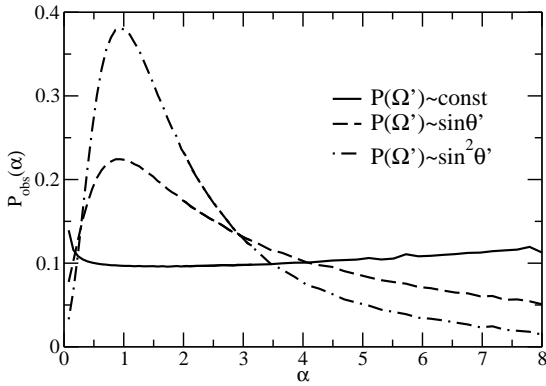


**Figure 2.** Probability (not normalized)  $P_{\text{obs}}(\alpha)d\Omega \propto P(\alpha)d(\Omega)/\Gamma_{\text{em}}^2$  that a minijet is observed at angle  $\alpha$  for different distributions  $P(\Omega')d\Omega'$  of direction of the minijets (in the jet rest frame).

Minijets pointing to larger angles are more broadly beamed. As a result, the probability that a blob is observed at an angle  $\theta$  depends weakly on  $\theta$ .

Out of  $N$  minijets forming in the jet, approximately  $N/\Gamma_{\text{co}}^2$  will be beamed at an observer located at any angle with respect to the jet axis. The observed duration and intensity of these flares will, however, depend on the observer's angle with respect to the jet axis, with on-axis observers seeing far more powerful flares. We quantify this point in the next section.

## 2.2 Dependence of observed properties of the minijets on the inclination to the jet axis

As we have shown in the previous section, the probability that a minijet emits within the observer's line of sight depends only weakly on the inclination of the observer with respect to the jet axis. However, the detectability of emission of a minijet depends on the luminosity of the source. The bolometric luminosity of a minijet is related to the total radiated energy of the minijet  $E$ , the solid angle

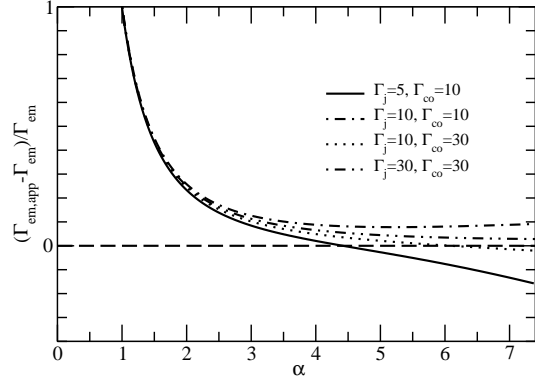


**Figure 3.** Fractional accuracy of approximate expression (4) of the bulk Lorentz factor of the minijet compared to the exact expressions (1) and (2) as function of inclination  $\alpha$ . The different curves correspond to different values of  $\Gamma_j$  and  $\Gamma_{\text{co}}$ . For  $\alpha \gtrsim 2$ , the approximate expression gives the correct answer within better than 20%.

$\Omega_{\text{em}}$  over which the emission takes place, and the observed duration  $\delta t_{\text{obs}}$  of the emission:  $L \simeq E/\Omega_{\text{em}}\delta t_{\text{obs}}$ . In the following we discuss how  $E$ ,  $\Omega_{\text{em}}$  and  $\delta t_{\text{obs}}$  depend on the inclination of the minijet.

The expressions (1) and (2) give the velocity of the minijet in the lab frame once the comoving angle  $\theta'$  is specified. Here, we derive much simpler, approximate expressions for the velocity and direction of motion of the minijet that points at  $\theta > 1/\Gamma_j$  (off the jet axis). In the following we express the various quantities as functions of the inclination  $\alpha$ . In the limit where  $\Gamma_j, \Gamma_{\text{co}} \gg 1$  and  $1 \lesssim \alpha \lesssim \Gamma_j, \Gamma_{\text{co}}$ , eq. (1) for the Lorentz factor of the blob becomes

$$\Gamma_{\text{em,app}} \simeq \frac{2\Gamma_j\Gamma_{\text{co}}}{\alpha^2}. \quad (4)$$

and eq. (2)

$$\theta = \frac{2}{\Gamma_j(\pi - \theta')}, \quad \text{or} \quad \alpha = \frac{2}{\pi - \theta'}. \quad (5)$$

In Fig. 3, we show the fractional error of expression (4) with respect to the exact one [eq. (1)] as function of inclination  $\alpha$  and for different values of  $\Gamma_j, \Gamma_{\text{co}}$ . For  $\Gamma_j, \Gamma_{\text{co}} \gtrsim 5$ , the approximate expression is rather accurate provided that  $\alpha \gtrsim 2$ . In the analytical estimates that follow we use the approximate expression (4).

From eq. (4), we find that a minijet moves relativistically towards the observer for a wide range of inclinations  $\alpha < (2\Gamma_j\Gamma_{\text{co}})^{1/2}$ . This leads to the possibility of emitters with high Doppler factor  $\delta \gg 1$  even in cases where the jet is misaligned by large angles  $\theta \gtrsim 30^\circ$ .

We assume that all the minijets are identical in a frame comoving with the jet and differ only in their orientation  $\theta'$ . Suppose that the energy of the minijets is  $\tilde{E}$  (in the minijet rest frame). When  $\theta \lesssim 1/\Gamma_j$  (i.e.,  $\alpha \lesssim 1$ ), a blob has lab-frame energy  $E_{\text{on}} = \Gamma_{\text{em}}\tilde{E} \sim \Gamma_j\Gamma_{\text{co}}\tilde{E}$  while for  $\theta > 1/\Gamma_j$  the energy of the minijet is  $E_{\text{off}} \sim 2\Gamma_j\Gamma_{\text{co}}\tilde{E}/\alpha^2 \sim 2E_{\text{on}}/\alpha^2$ . Since the emission of the minijet takes place within a solid angle  $\Omega_{\text{em}} \sim 1/\Gamma_{\text{em}}^2$ , the emission from minijets that point off the jet axis is less beamed than that of on-axis ones:  $\Omega_{\text{off}} \sim \alpha^4\Omega_{\text{on}}/4$ .

The observed timescale of emission from a minijet depends on the size of the blob, its bulk Lorentz factor, and the radiative mechanism or the duration of the reconnection event. Identical blobs (i.e., of the same size, density, magnetic field strength)

that emit through the synchrotron and synchrotron-self-Compton (SSC) mechanisms have the same emission timescale  $\delta t$  in the rest frame of the minijet. The observed duration of the blob emission is  $\delta t_{\text{obs}} = \delta t / \Gamma_{\text{em}}$ . Thus, the duration of the flare for an off axis observer is<sup>2</sup>  $\delta t_{\text{off}} \sim \alpha^2 \delta t_{\text{on}} / 2$ . This expression shows that the timescale of emission becomes longer when the jet is viewed from larger inclination. On the other hand, the dependence on  $\alpha$  is rather moderate. If minijets result in the very rapidly evolving flares of the blazars Mrk 501 and PKS 2155-304 with  $\delta t_{\text{on}} \sim 0.1 R_g / c$  (Giannios et al. 2009), misaligned jets with  $\alpha \sim$  a few can also lead to rather short variability timescales  $\delta t_{\text{off}} \sim R_g / c$ .

Combining the above estimates, if the minijets emit through synchrotron and SSC, the bolometric luminosity during the flare of an off-axis blob is

$$L_{\text{off}} \sim \frac{E}{\Omega_{\text{em}} \delta t_{\text{obs}}} \sim \frac{16 L_{\text{on}}}{\alpha^8}. \quad (6)$$

Although the  $\alpha^8$  dependence is very steep, making flares from misaligned jets rather weak, it is still possible to observe them from nearby sources.

The gamma-ray emission from the minijets may not be dominated by SSC, but by inverse Compton scattering of an external source of seed photons, provided that a powerful enough source exists. The accretion disk and the broad line region have been frequently considered in this respect (Dermer, Schlickeiser & Mastichiadis (1992); Sikora, Begelman & Rees (1994)). In the jets-in-a-jet model discussed here, soft (synchrotron) emission emitted at a different location in the jet can also be considered as an external photon field *from the point of view* of the minijet. Such a photon field, approximately isotropic in the rest frame of the jet, may be connected to the process responsible for the quiescent jet emission or may come from the averaged synchrotron emission of all the minijets forming during the flaring activity of the jet. One can show that the expression (6) for the dependence of the blob's luminosity on its inclination to the jet axis holds for the external inverse Compton mechanism, *provided that* the photon field is approximately isotropic in the rest frame of the jet. On the other hand, if there is a significant source of soft radiation coming from the base of the jet (e.g., the accretion disk), the scaling (6) fails.

As we shall see in the next section, the observed soft emission coming from the nucleus of M87 (associated with the accretion disk and/or the inner jet) provides plenty of seed photons to be inverse Compton scattered in the minijet. External inverse Compton appears to be an important mechanism for the gamma-ray emission from this source.

### 3 APPLICATION TO THE FLARING TEV EMISSION FROM M87

The nucleus of M87 contains a  $M \approx 3 \times 10^9 M_{\odot}$  black hole (corresponding to light-crossing time of  $R_g / c \sim 1.5 \times 10^4$  sec) measured from gas kinematics on scales of  $10^2$ 's of parsecs (Macchetto et al. 1997). The M87 jet, believed to originate from the black hole, has been extensively observed from radio to TeV and from sub-pc to kpc scales.

Modeling of the kpc-scale interaction of the jet with the external medium constrains the properties of the jet. Though rather

model dependent, the jet inclination is estimated to be  $\theta \sim 30^\circ$  with respect to the line of sight, the bulk Lorentz factor of the jet  $\Gamma_j \sim 5$  and the kinetic luminosity  $L_{j,\text{true}} \sim 10^{43}$  erg/sec (Bicknell & Begelman 1996; Reynolds et al. 1996; Owen et al. 2000; Stawarz et al. 2006; Bromberg & Levinson 2009).

The nucleus of M87 and the knot HST-1 (about 60 pc away from the nucleus) are active with luminosity of order of  $\sim 10^{41}$  erg/sec each over a wide range of wavelengths (from IR to gamma-rays; see, e.g., Sparks, Biretta & Macchetto 1996; Perlman et al. 2001). Both the nucleus and the knot HST-1 have shown variability in X-rays and optical on timescales ranging from months to years (see, e.g., Harris et al. 2009) indicating rather compact emitting regions. During 2005, M87 was luminous in the TeV band with isotropic  $L_{\text{TeV}} \sim 3 \times 10^{40}$  erg/sec and exhibited flares evolving on  $\sim 2$ -day timescales (Aharonian et al. 2006). The poorer angular resolution in TeV energies allows for both the nucleus and HST-1 as possible sources of the high-energy emission. During the 2005 TeV flaring, HST-1 was at its peak of its optical and X-ray activity (exceeding the nuclear emission), making the knot a promising candidate for the origin of the flares (Cheung et al. 2007). In February 2008, TeV flaring on  $\sim 1$  day timescales was observed from M87, this time not associated with high activity from the knot HST-1. The correlation of TeV and X-ray fluxes on month to year timescales in the nucleus favors the nuclear region as the source of the TeV flares (Acciari et al. 2008; Harris et al. 2009). Even more convincingly, the 2008 TeV flaring was followed by new radio blobs moving outward from only  $\sim 100 R_g$  from the black hole, suggesting that the gamma-ray flare comes from very close to the black hole (Accuari et al. 2009).

If the jet of M87 is misaligned (pointing at an angle  $\theta \sim 30^\circ$  away from the observer), the associated Doppler factor is  $\delta = 1/\Gamma_j(1 - v_j \cos \theta) \sim 1$ . In this case relativistic effects do not contribute to reduce variability timescales. The physical size of the TeV source is very compact,  $l_{\text{em}} \lesssim ct_v \sim 5 R_g$ . This points to the possibility that the emission takes place in the vicinity of the black hole. TeV emission coming directly from the magnetosphere of the black hole is proposed by Neronov & Aharonian (2007; see also Levinson 2000). A potential problem with this interpretation of the TeV emission is that infrared and optical radiation originating from the accretion disk may be strong enough to absorb TeV photons. The modeling of the emission of the accretion flow and fits to observations of the nuclear emission indicate that TeV emission is absorbed if produced at  $R \lesssim 20 R_g$  (Li et al. 2009). During the flaring, the high-energy emission extends up to at least  $\sim 10$  TeV with the TeV spectrum well described by a power-law model with a photon-number index of  $\Gamma \sim -2.3$  (Aharonian et al. 2006; Albert et al. 2008). There is no evidence for absorption of the TeV emission, suggesting that the emission takes place at  $R_{\text{em}} \gtrsim 20 R_g$ .

It has also been proposed that the TeV flares come directly from the inner (pc-scale) regions of a misaligned jet. These models are more complex than single-zone SSC models and either invoke jet deceleration on sub-pc scales (Georganopoulos et al. 2005) or a multi-zone configuration with a fast spine and slower outer layer (Tavecchio & Ghisellini 2008). One weakness of these models is that they tend to produce steeper TeV spectra than those observed, because of absorption by the dense soft (synchrotron) photon field along the line of sight.

Our jets-in-a-jet picture provides a way out of these difficulties. While the jet is misaligned with respect to the observer, some minijets point outside the jet emission cone and in the direction to the observer. These "off-axis" minijets move relativistically toward the observer and can be compact, resulting in TeV flares with short

<sup>2</sup> If the observed timescale of emission is determined by the duration of the reconnection event, the duration of the flare for an off-axis observer can similarly be shown to be  $\delta t_{\text{off}} \sim \alpha^2 \delta t_{\text{on}} / 2$ .

variability timescales. Furthermore, the relativistic beaming toward the observer allows the TeV emission to escape the production site without being significantly absorbed.

### 3.1 Jets in the jet of M87

For more quantitative estimates we consider a jet with (isotropic) luminosity  $L_{j,\text{iso}}$  that moves with bulk  $\Gamma_j$ . The jet is assumed to be strongly magnetized with a Poynting-to-kinetic flux ratio (magnetization)  $\sigma \gg 1$ . As reference values, we use  $\Gamma_j = 5$  and  $\sigma = 100$ . The isotropic equivalent jet luminosity is estimated to be  $L_{j,\text{iso}} = 4\Gamma_j^2 L_{j,\text{true}} \sim 10^{45}$  erg/s. The energy density and magnetic field strength in the jet as function of radius are (e.g., Giannios et al. 2009):

$$e'_j = L_{j,\text{iso}}/4\pi r^2 c \Gamma_j^2 = 0.05 L_{j,45} r_2^{-2} \Gamma_{j,5}^{-2} \text{ erg/cm}^3, \quad (7)$$

and

$$B'_j = \sqrt{4\pi e'_j} = 0.8 L_{j,45}^{1/2} r_2^{-1} \Gamma_{j,5}^{-1} \text{ Gauss}, \quad (8)$$

where  $A = 10^3 A_x$  and the spherical radius is  $R = r \cdot R_g$  with  $R_g = 4.5 \times 10^{14}$  cm, corresponding to the gravitational radius of a black hole of  $3 \times 10^9 M_\odot$ .

We assume that a fraction of the magnetic energy of the jet is occasionally dissipated through reconnection. Our picture for relativistic reconnection is the relativistic generalization of Petschek-type reconnection worked out by Lyubarsky (2005; see also Watanabe & Yokoyama 2006; Zenitani, Hesse & Klimas 2009 for relativistic MHD simulations that support this picture). High- $\sigma$  material is advected into the reconnection region where the release of magnetic energy takes place. Part of the dissipated magnetic energy serves to give bulk acceleration to a pair of minijets that move in opposite directions (in the rest frame of the jet) and the rest to accelerate particles in the minijets. We explore the possibility that emission from minijets results in the observed flaring activity.

In this model, the material can leave the reconnection region with bulk  $\Gamma_{\text{co}}$  close to the Alfvén speed of the upstream plasma:  $\Gamma_{\text{co}} \sim \sqrt{\sigma} \approx 10\sigma_2^{1/2}$  in the rest frame of the jet (Petschek 1964; Blackman & Field 1994; Lyutikov & Uzdensky 2003; Lyubarsky 2005). The energy density in the minijet is (Lyubarsky 2005)  $\tilde{e}_{\text{em}} \sim e'_j = L_{j,\text{iso}}/4\pi r^2 c \Gamma_j^2 = 0.05 L_{j,45} r_2^{-2} \Gamma_{j,5}^{-2} \text{ erg/cm}^3$ .

Even though we consider a Poynting flux-dominated jet, the (downstream) emitting region is not necessarily magnetically dominated since a large part of the magnetic energy dissipates in the reconnection region. This has important implications for the resulting spectra. Actually, Lyubarsky (2005) shows that material leaves the reconnection region with  $\Gamma_{\text{co}} \sim \sqrt{\sigma}$  for sufficiently small guide field. In this case, the magnetization of the minijet (downstream plasma) is  $\sigma_{\text{em}} \equiv \tilde{B}_{\text{em}}^2/4\pi\tilde{e}_{\text{em}} < 1$ , and the magnetic field in the minijet rest frame is parameterized as  $\tilde{B}_{\text{em}} = \sqrt{\sigma_{\text{em}} 4\pi\tilde{e}_{\text{em}}} = 0.8\sigma_{\text{em}}^{1/2} L_{j,45}^{1/2} r_2^{-1} \Gamma_{j,5}^{-1} \text{ Gauss}$ . If the guide field of the upstream plasma is stronger, the minijet is strongly magnetized with  $\sigma_{\text{em}} \gtrsim 1$ , and slower,  $\Gamma_{\text{co}} < \sqrt{\sigma}$ . Furthermore, only a fraction  $\sim 1/(1 + \sigma_{\text{em}})$  of the magnetic energy is dissipated in the reconnection region, leading to a rather weaker and slower minijets. Here we focus on fast minijets characterized by  $\sigma_{\text{em}} \lesssim 1$ .

### 3.2 Particle distribution

Assuming an electron-proton jet, the plasma coming into the reconnection region (the upstream) contains  $\sim \sigma m_p c^2$  magnetic energy

per particle. Out of this energy a fraction  $\sqrt{\sigma}$  goes into bulk motions with the rest being available to accelerate/heat particles. In the frame of the reconnection jet (minijet), the available energy per particle is  $\sim \sqrt{\sigma} m_p c^2$ . If electrons receive an appreciable fraction of the released magnetic energy  $f \sim 0.5$ , they are heated to characteristic thermal  $\gamma$  factor

$$\gamma_{e,\text{ch}} \sim f \sqrt{\sigma} m_p / m_e \sim 10^4 f_{1/2} \sigma_2^{1/2}, \quad (9)$$

assumed to be isotropic in the blob rest frame.

In the context of the leptonic emission model discussed here, electrons of at least  $\sim 10$  TeV (in the lab frame) are needed to potentially explain the observed emission that extends up to  $\sim 10$  TeV. This means that the random component of the electron distribution should extend to  $\gamma_e > 2 \times 10^7 / \Gamma_{\text{em}} \gg \gamma_{e,\text{ch}}$  (in the minijet frame), where  $\Gamma_{\text{em}}$  is the bulk Lorentz factor of the minijet. It is thus clear that electrons need to be accelerated well above the characteristic Lorentz factor  $\gamma_{e,\text{ch}}$ . For simplicity, we will assume that the electrons follow a power-law distribution that extends to  $\gamma_e \gg \gamma_{e,\text{ch}}$ . It remains to be shown that relativistic reconnection can lead to such a particle distribution.

Since, for the parameters relevant to the jet of M87, particles with  $\gamma_e \gtrsim \gamma_{e,\text{ch}}$  are fast cooling (because of synchrotron and, mainly, inverse Compton emission; see next section), we consider emission coming from a rather steep particle distribution with  $p \gtrsim 3$ . The particle distribution has a maximum cutoff  $\gamma_{\text{max}}$ . In our discussion,  $\gamma_{\text{max}}$  is not important (provided that it is high enough to produce  $\sim 10$  TeV photons through inverse Compton) and will be set to  $\gamma_{\text{max}} \rightarrow \infty$ .

### 3.3 Radiation mechanisms

The minijet contains energetic electrons that emit through synchrotron and synchrotron-self-Compton and, possibly, external inverse Compton (EIC) mechanisms. We consider *any* source external to the minijet contributing seed photons that are scattered by the minijet as an EIC source. Following this definition, not only disk emission but also soft photons originating from other parts of the jet that interact with the minijet are labeled as EIC sources.

In this Section, we explore the emission from a minijet for parameters of the model relevant to M87 (i.e., we set  $\theta = 30^\circ$ ,  $\Gamma_j = 5$ ). Other parameters of the model (i.e., magnetization of the jet, radius of formation of the minijet) are less constrained. Since we model M87 as a misaligned blazar, for illustration we set these parameters to values inferred from modeling of Mrk 501 and PKS 2155-304 (Giannios et al. 2009). The Lorentz factor of the minijet in the rest frame of the jet is, therefore, set to  $\Gamma_{\text{co}} = \sqrt{\sigma} = 10$ . For these parameters, using eqs. (1), (2) we find that the minijet moves with  $\Gamma_{\text{em}} = 12$ . The formation of the minijet is assumed to take place at  $R_{\text{em}} = 100R_g$  and the magnetization of the plasma within the minijet is set to  $\sigma_{\text{em}} = 1/3$  (though different values of  $\sigma$  and  $\sigma_{\text{em}}$  are explored as well). From the observed luminosity ( $L_f \sim 10^{42}$  erg/sec) and duration ( $T_f \sim 10^5$  sec) of the TeV flares, we can estimate the lab-frame energy contained in the minijet  $E_{\text{em}} \sim L_f T_f / 4\Gamma_{\text{em}}^2 f \sim 5 \times 10^{44}$  erg and the typical length scale of the emitting region is  $l_{\text{em}} \sim (E_{\text{em}} / \Gamma_{\text{em}} \tilde{e}_{\text{em}})^{1/3} \sim 10^{15}$  cm. The minijet can be easily powered by the M87 jet of  $L_{j,\text{true}} \sim 10^{43}$  erg/sec. In the following, we show that the minijet emits its energy efficiently in the  $\sim$  TeV energy range.

The synchrotron emission of electrons with random Lorentz factor  $\gamma_{e,\text{ch}}$  takes place at observed energy  $\nu_{\text{syn}} \sim \Gamma_{\text{em}} \gamma_e^2 \nu_c \approx 5 L_{j,45}^{1/2} \sigma_2^{3/2} f_{1/2}^2 r_2^{-1} \text{ eV}$  if the minijet points at us, where  $\nu_c$  is the electron cyclotron frequency. The self-Compton emission appears

at  $v_{\text{SSC}} \sim \gamma_e^2 v_{\text{syn}} \approx 0.5 L_{j,45}^{1/2} \sigma_2^{5/2} f_{1/2}^4 r_2^{-1}$  GeV. Higher energy emission is expected by particles with  $\gamma_e > \gamma_{e,\text{min}}$ .

In addition to the synchrotron emission in the minijet, ambient photon fields present in the nucleus of M87 are also a source of seed photons to be upscattered by the minijet. Some of these soft photons come from the accretion flow (Di Matteo et al. 2003; Li et al. 2009) and the rest from the inner jet. The observed nuclear emission has a flat  $Ef(E)$  spectrum in the range  $\sim 0.01 - 10$  eV with integrated luminosity  $\sim 3 \times 10^{41}$  erg/sec declining at  $E \lesssim 0.01$  eV and  $E \gtrsim 10$  eV (e.g., Li et al. 2009). The nuclear emission has been resolved down to  $\sim 20R_g$  in the radio (see, e.g., Spencer & Junor 1986; the radio emission is believed to come from the jet). The resolution is poorer in shorter wavelengths, corresponding to an upper limit to the size of the nucleus of  $\sim 100R_g$  in the mm and  $\sim 3 \times 10^4 R_g$  in the infrared (Whysong & Antonucci 2004).

The *observed* emission from the nucleus competes with the synchrotron emission from the minijet as sources of seed photons to be inverse-Compton scattered in the minijet. A conservative estimate for the role of external soft photons comes from assuming that they are emitted isotropically from a region close to the black hole. If, on the other hand, a large fraction of the observed soft photons comes from the jet (i.e. they are emitted isotropically in the jet frame), their intensity along the jet axis is much larger than that estimated assuming isotropic emission from the inner disk.

If the soft photon field is emitted isotropically from a region with length scale  $R_{\text{soft}}$ , the typical angle  $\theta_{\text{int}}$  at which the soft photons interact with the bulk motion of the minijet depends on the ratio  $R_{\text{soft}}/R_{\text{em}}$ . For  $R_{\text{soft}}/R_{\text{em}} \ll 1$ , the interaction angle equals approximately the inclination of the minijet  $\theta_{\text{int}} \sim \theta \sim 30^\circ$  while for  $R_{\text{soft}}/R_{\text{em}} \lesssim 1$ , the interaction angle is larger,  $\theta_{\text{int}} \sim 60^\circ$ . The energy density of the external photon field at the location of the minijet is  $\tilde{U}_{\text{ph}} \sim (1 - \beta_{\text{em}} \cos \theta_{\text{int}}) \Gamma_{\text{em}}^2 L_{\text{soft}} / 4\pi c R_{\text{em}}^2 = 0.04(1 - \beta_{\text{em}} \cos \theta_{\text{int}}) \Gamma_{\text{em},10}^2 L_{s,41.5} r_2^{-2}$  erg/cm<sup>3</sup> (in the rest frame of the minijet), which appears to be of the same order of magnitude as that of the magnetic field,  $\tilde{U}_{\text{B}} = 8 \times 10^{-3} L_{j,45} \sigma_{\text{em},1/3} r_2^{-2} \Gamma_{j,5}^{-2}$  erg/cm<sup>3</sup>. It should be noted that the expressions for  $\tilde{U}_{\text{ph}}$  and  $\tilde{U}_{\text{B}}$  hold for  $\sigma_{\text{em}} \lesssim 1$ . For  $\sigma_{\text{em}} \gtrsim 1$  the magnetic energy density  $\tilde{U}_{\text{B}}$  saturates to a value that is independent of  $\sigma_{\text{em}}$ , while for  $\sigma_{\text{em}} \gg 1$ , no minijet forms since the outflow from the reconnection region is expected to be slow and weak (since most of the magnetic energy is not dissipated by reconnection).

For reasonable range of the parameters, either SSC or EIC can dominate the production of the gamma rays. First, we explore parameters for which synchrotron seed photons and SSC dominate the bulk of the emission. We set  $\sigma_{\text{em}} \sim 1$  and assume a very compact emission region for the disk photons:  $R_{\text{soft}}/R_{\text{em}} \ll 1$ . The bulk Lorentz factor of the minijet is taken to be rather modest,  $\Gamma_{\text{em}} = 8$  (by setting  $\sigma = 50$ ). Having specified the properties of the minijet and of the ambient radiation field, we proceed with the calculation of the resulting spectra. We calculate the synchrotron emission from a power-law distribution of relativistic electrons using standard expressions. The SSC and EIC emission are calculated using the  $\delta$ -function approximation for single electron emission. Klein-Nishina effects on the electron scattering are approximated by using a step function for the energy dependence of the cross section:  $\sigma = \sigma_T$ , for  $\gamma_e h\nu / m_e c^2 < 3/4$  and  $\sigma = 0$  otherwise (see, for example Tavecchio, Maraschi & Ghisellini 1998 and Coppi & Blandford 1990 for discussion on the accuracy of this method).

The resulting spectra are shown in Fig. 4. Here we ignore any absorption of the TeV emission due to pair creation (discussed in the next section). The inverse Compton peak of the  $Ef(E)$  spectrum  $E_p = \Gamma_{\text{em}} \gamma_{e,\text{ch}} m_e c^2$  corresponds to the inverse Compton emission

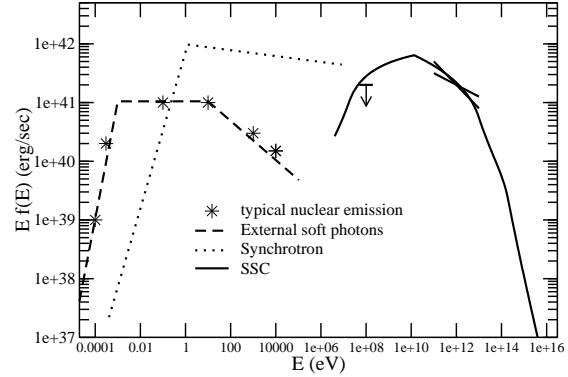


**Figure 4.** Synchrotron (dotted line) and inverse Compton (solid line) emission from a minijet forming at  $R_{\text{em}} = 100R_g$  and beaming at an angle  $\theta \sim 30^\circ$  with respect to the axis of the jet of M87. The magnetization of the minijet is set to  $\sigma_{\text{em}} = 1$  and a power-law electron distribution is assumed with index  $p = 3.1$ . The observed emission from the nucleus is sketched with the dashed line and is assumed to come from a region  $R_{\text{soft}} \ll R_{\text{em}}$ . The black bow-tie reports the TeV spectrum observed during the early 2008 flare (Albert et al. 2008). The EGRET  $2\sigma$  upper limit is also shown (Sreekumar et al. 1996).

from electrons with the characteristic Lorentz factor  $\gamma_{e,\text{ch}}$ . Since the peak is located below the working range of the Cherenkov telescopes,  $E_p \lesssim 100$  GeV (Aharonian et al. 2006; Albert et al. 2008), we have the constraint that  $\Gamma_{\text{em}} \gamma_{e,\text{ch}} \lesssim 2 \times 10^5$ . Above the peak, the TeV spectrum is rather flat with photon-number index  $\Gamma \approx -2.3$ . The TeV spectrum depends on the index  $p$  of the electron distribution (set to  $p = 3.1$ ). The TeV emission becomes harder for lower  $p$  and vice versa. At  $E \sim 10^{13}$  eV the spectrum steepens. Photons observed at  $E \gtrsim 10^{13}$  eV (i.e.,  $E \gtrsim 10^{12}$  eV in the rest frame of the minijet) mainly come from scattering in the Thomson regime of optical synchrotron photons (near-IR in the minijet frame), the energy density of which drops rapidly with decreasing energy.

The slope of the TeV emission spectrum is compatible with that observed during the fast TeV flaring in 2005 (Aharonian et al. 2006) and 2008 (Albert et al. 2008). At the same time the synchrotron emission is clearly pronounced in the optical, UV and X-rays, far exceeding (by a factor of 10-30) the typical nuclear emission. Note that, within the one-zone SSC model for the TeV emission discussed here, the synchrotron component peaks close to the optical and extends up to the hard X-rays rather independently of the adopted parameters. For photons to be upscattered to energies  $E \gtrsim 10$  TeV in the Thomson regime, the synchrotron emission cannot peak much above the optical wavelengths. Furthermore, the electrons with random  $\gamma_e \sim 10^6$  needed to produce the  $E \gtrsim 10$  TeV emission emit into the hard X-ray regime through synchrotron (for the magnetic field strength in the minijet of order 1 Gauss predicted by the model). Since powerful optical and X-ray flares with  $\sim 1$  day timescales have not been observed in the nucleus despite the regular monitoring of M87, we consider the SSC interpretation of the TeV emission unlikely.

The synchrotron component of the minijet is weaker when  $\sigma_{\text{em}} < 1$ . This brings us to the parameter space for which the EIC mechanism plays a more important role. We set  $\sigma_{\text{em}} = 1/3$  (or smaller) and assume an extended region for the external emissions:  $R_{\text{soft}}/R_{\text{em}} \lesssim 1$ . The bulk Lorentz factor is set to  $\Gamma_{\text{em}} = 12$

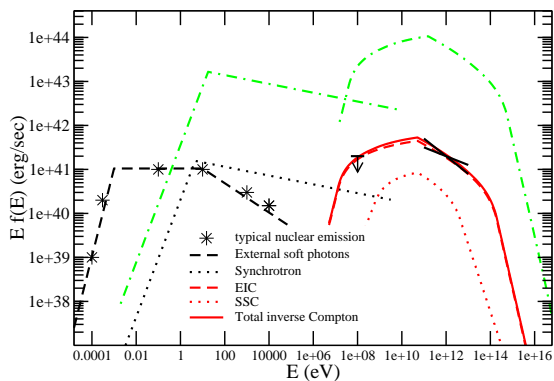


**Figure 5.** Same as in Fig. 4 but with the magnetization of the minijet set to  $\sigma_{\text{em}} = 1/3$  and the observed emission from the nucleus assumed to come from a larger region,  $R_{\text{soft}} \lesssim R_{\text{em}}$ . A power-law electron distribution is assumed with index  $p = 3.2$ . For these parameter the EIC mechanism dominates the gamma-ray emission. The green dash-dotted lines show the synchrotron and inverse Compton emission from an identical blob beaming within the jet axis as observed by an observer located at an angle  $\theta = 1/\Gamma_j = 11^\circ$  (with respect to the jet axis).

(by setting  $\sigma = 100$ ). The resulting spectra are shown in Fig. 5, where one can see that EIC dominates the GeV-TeV emission. For smaller values of  $\sigma_{\text{em}}$  the synchrotron and SSC components become weaker but the TeV emission remains practically the same. The TeV spectrum is rather well described with a power-law model with photon-number index  $\Gamma \simeq -2.3$ . The slope of the TeV spectrum depends on the spectrum of the soft seed photons (observed to be  $F_{\text{soft}}(E) \propto E^{-1}$ ) and the index  $p$  of the electron distribution (set to  $p = 3.2$ ). At  $E \sim 3 \times 10^{14}$  eV the spectrum steepens because the energy density of the available soft seed photons with  $E_s \lesssim 10^{-3}$  eV for scattering in the Thomson regime drops rapidly with decreasing energy.

The slope of the TeV emission spectrum is compatible with that observed during the fast TeV flaring in 2005 (Aharonian et al. 2005) and 2008 (Albert et al. 2008). During the TeV flares the  $\sim 100$  MeV flux approaches the upper limits set by *EGRET* (see Fig. 5). If M87 is currently in a high GeV-TeV state, we predict that *FERMI* should soon have a significant detection of the nuclear emission.

During flares, the synchrotron emission from the minijet dominates the nuclear emission in the X-rays, provided that  $\sigma_{\text{em}} \gtrsim 0.1$ . In this case, simultaneous X-ray flares of moderate strength are expected. Unfortunately, there have been no X-ray observations strictly simultaneous with the TeV flares. On the other hand, monitoring of the nucleus in X-rays in 2008 revealed that it was in a high X-ray state around the time of the TeV flares. Simultaneous multi-wavelength observations can greatly constrain magnetization of the emitting region.

In Fig. 5, we also show for comparison the emission expected from M87 if it were observed at an inclination  $\theta = 1/\Gamma_j \sim 11^\circ$ , i.e., at  $\alpha = 1$ . In that case, the flares would be more powerful, powered by minijets emitting within the jet axis, and have observed durations of  $\sim$ several hours. The synchrotron emission would peak in the extreme UV and the inverse Compton component at  $\sim 100$  GeV. Both the timing and spectral properties would look similar to those of a low luminosity, high-frequency BL Lac (HBL) object.

Note, however, that in HBLs the inverse Compton peak is typically not as pronounced with respect to the synchrotron one as that of Fig. 5.

### 3.3.1 Escape of the TeV photons

The spectrum of the TeV emission from M87 does not show any signature of absorption up to  $\sim 10$  TeV. In this section, we examine the conditions under which the TeV emission from a misaligned minijet escapes pair creation in the region where it is produced.

The dominant source of infrared-optical photons that can pair create with the TeV photons is the ambient nuclear emission<sup>3</sup>. The size of the emitting region (which likely depends on the wavelength of the emission) and the location and direction of the minijet determine the typical angle  $\theta_{\text{int}}$  at which the TeV photons interact with soft photons. For a rough estimate of this angle we set  $R_{\text{soft}} \lesssim R_{\text{em}}$ , resulting in  $\theta_{\text{int}} \sim 60^\circ$ . The pair-creation cross section peaks at  $\sigma_{\gamma\gamma} \sim \sigma_T/5$  for photons with total energy  $E_{\text{CM}} \sim 4m_e c^2$  in the center of mass frame. The center-of-mass energy of a hard photon  $E_h$  and a soft photon  $E_s$  that form an angle  $\theta_{\text{int}} \sim 60^\circ$  is  $E_{\text{CM}} = \sqrt{2E_h E_s (1 - \cos \theta)} \sim \sqrt{E_h E_s}$ . The  $\gamma\gamma$  annihilation cross section peaks at soft photon energy  $E_s \simeq 4/E_{h,1\text{TeV}}$  eV. Since the number density of soft photons increases at the lower energies,  $\sim 10$  TeV photons are the most likely to be absorbed by  $\sim 0.4$  eV target soft photons. The number density of soft photons is  $N_{\text{target}} = L_{\text{IR}}/4\pi R_{\text{em}}^2 c E_s$ , where  $L_{\text{IR}} \sim 10^{41}$  erg/sec is the near-infrared luminosity of the nucleus (see Figs. 4, 5). Thus, the annihilation optical depth is

$$\tau_{\gamma\gamma} = N_{\text{target}} \sigma_{\gamma\gamma} R_{\text{em}} \simeq 1 L_{\text{IR},41} E_{h,10\text{TeV}} / r_2. \quad (10)$$

From this expression we conclude that for  $R_{\text{soft}} \lesssim R_{\text{em}}$ , the  $\sim 10$  TeV photons marginally avoid significant attenuation if the minijet forms at  $R_{\text{em}} \sim 100 R_g$ . If, however,  $R_{\text{soft}}$  is much smaller than  $R_{\text{em}}$  then escape is possible from smaller radii.

## 4 DISCUSSION/CONCLUSIONS

M87 is a well studied case of a misaligned AGN jet. Both the nucleus of M87 and the knot HST-1 have variable emission on timescales of weeks to months, in particular in the X-rays (e.g., Harris et al. 2009). More impressively, M87 reveals compact TeV emitting regions by producing flares on  $\sim 1$  day timescales (Aharonian et al. 2006; Albert et al. 2008). VLBI observations during and after the 2008 TeV flares showed the ejection of two blobs within a distance of  $\sim 100 R_g$  from the black hole, strongly suggesting the nucleus as the source of the flare (Acciari et al. 2009).

The TeV flares may originate from the magnetosphere of the black hole (Levinson 2000; Neronov & Aharonian 2007) or a complex jet geometry (spine/layer interaction [Tavecchio & Ghisellini 2008]; collimating jet [Lenain et al. 2008]; decelerating jet [Georganopoulos et al. 2005]). Still, in models in which the jet is misaligned with respect to our line of sight, the Doppler factor of the emitting material is  $\delta \sim 1$ , implying the need to explain a very compact emitting region of length scale  $l_{\text{em}} \lesssim 5 R_g$  and the lack of TeV absorption.

<sup>3</sup> The synchrotron photons from the minijet may, in principle, also contribute to the TeV absorption. In practice, however, the strong beaming of the minijets toward the observer guarantees that the synchrotron photons can be ignored as a source of opacity.

Rapid gamma-ray flaring has been observed frequently in blazars. Mrk 501 and PKS 2155-304 show powerful flares at TeV energies with duration of several minutes, much shorter than the light crossing time of their central black holes (Aharonian 2007; Albert et al. 2007). This extremely fast flaring suggests that the flares do not reflect variability of the central engine in these jets but is connected to interactions within the jet, which lead to compact emitting regions and potentially relativistic motions in the rest frame of the jet.

In this line of argument, we have previously proposed a jets-in-jet model for blazars (Giannios et al. 2009). Minijets, driven by magnetic reconnection and moving relativistically within the main jet, can power the fast evolving flares, make them transparent at TeV energies, and explain why the jet as a whole appears much slower. The reconnection may be triggered by MHD instabilities in the jet (like kinks) and/or reversals of the polarity of the magnetic field in the magnetosphere of the black hole or in the inner disk. When a field reversal takes place, interactions/collisions of parts of the jet with opposite polarity can lead to very efficient release of magnetic energy via magnetic reconnection.

Reconnection within the jet produces two oppositely directed (in the jet's frame) minijets. One of them always points within the jet angle and is observable in blazars because their jets point at us. The other minijet (its counterpart) points outside the jet opening angle and is potentially observable to off-axis observers in case of misaligned jets, e.g., M87 or Cen A (Aharonian et al. 2009).

The TeV flaring of M87 can be understood in this context. Furthermore, we predict that if M87 is currently in a high GeV-TeV state, *FERMI* should soon have a significant detection of the nuclear emission. Finally, if viewed on-axis, M87 would look like a fairly regular high peaked BL-Lac object with TeV (and possibly optical/Xray) flares of several hours.

The high-energy emission from the minijets comes during their formation/ejection and/or the (short) cooling timescale associated with the TeV emitting particles. The observed TeV flares are likely part of a general increase of minijet events in the jet, most of which we do not see because they are beaming away from us. On a longer timescale, the minijets interact with the rest of the jet and are slowed down (with respect to the jet). During this interaction phase, shocks are expected to form, resulting in further acceleration of particles that can power an 'afterglow' emission. Interestingly the Acciari et al. (2009) VLBI observations that followed the February 2008 flaring of M87 showed the ejection of radio blobs from the nuclear region. It is tempting to associate these blobs with the collective afterglows from minijets brought to our view after their deceleration to the jet mean motion.

By analogy with the  $\sim 5$  min flares seen from Mrk 501 and PKS 2155-304, one might expect even faster evolving flares from M87 than the observed  $\sim 1$  day ones. Taking into account that the black hole of M87 is a factor of  $\sim 3$  larger than those of Mrk 501 and PKS 2155-304 and that the large inclination of the M87 jet dilutes timescales by a factor of  $\alpha^2 \sim 10$ , one could still expect flares evolving in as short as 2 – 3 hours from M87.

#### ACKNOWLEDGMENTS

DG acknowledges support from the Lyman Spitzer Jr. Fellowship awarded by the Department of Astrophysical Sciences at Princeton University. DG acknowledges the support of the NORDITA program on *Physics of relativistic flows* during which part of this work was completed. DU is supported by National Science Founda-

tion Grant No. PHY-0821899 (PFC: Center for Magnetic Self-Organization in Laboratory and Astrophysical Plasmas). MCB acknowledges support from NASA, via a *Fermi Gamma-ray Space Telescope* Guest Investigator grant.

#### REFERENCES

- Acciari V. A. et al., 2008, *ApJ*, 679, 397  
 Acciari V. A. et al., 2009, *Science*, 325, 444  
 Aharonian F. et al., 2006, *Science*, 314, 1424  
 Aharonian F. et al., 2007, *ApJ*, 664, L71  
 Aharonian F. et al., 2009, *ApJ*, 695, L40  
 Albert J. et al., 2007, *ApJ*, 669, 862  
 Albert J. et al., 2008, *ApJ*, 685, L23  
 Appl S., Lery T., Baty H., 2000, *A&A*, 355, 818  
 Begelman M. C., 1998, *ApJ*, 493, 291  
 Begelman M. C., Fabian A. C., Rees M. J., 2008, *MNRAS*, 384, L19  
 Bicknell G. V., Begelman M. C., 1996, *ApJ*, 467, 597  
 Biretta J. A., Zhou F., Owen F. N., 1995, *ApJ*, 447, 582  
 Blackman E. G., Field, G. B., 1994, *Physical Review Letters*, 72, 494  
 Blandford R. D., 2002, in Gilfanov M., Sunyaev, R., Churazov, E., eds, *Lighthouses of the Universe: The Most Luminous Celestial Objects and Their Use for Cosmology*. Springer, Berlin, p. 381  
 Bromberg O., Levinson A., 2009, *ApJ*, 699, 1274  
 Cheung C. C., Harris D. E., Stawarz Ł., 2007, *ApJ*, 663, L65  
 Coppi P. S., Blandford R. D., 1990, *MNRAS*, 245, 453  
 Dermer C. D., Schlickeiser R., Mastichiadis A., 1992, *A&A*, 256, L27  
 Di Matteo T., Allen S. W., Fabian A. C., Wilson A. S., Young A. J., 2003, *ApJ*, 582, 133  
 Eichler D., 1993, *ApJ*, 419, 111  
 Georganopoulos M., Perlman E. S., Kazanas D., 2005, *ApJ*, 634, L33  
 Gebhardt, K., & Thomas, J. 2009, *ApJ*, 700, 1690  
 Giannios D., Spruit H. C., 2006, *A&A*, 450, 887  
 Giannios D., Uzdensky D. A., Begelman M. C., 2009, *MNRAS*, 395, L29  
 Giroletti M. et al., 2004, *ApJ*, 600, 127  
 Harris, D. E., Cheung, C. C., Stawarz, Ł., Biretta, J. A., & Perlman, E. S. 2009, *ApJ*, 699, 305  
 Lazar A., Nakar E., Piran T., 2009, *ApJ*, 695, L10  
 Lenain J.-P., Boisson C., Sol H., Katarzyński K., 2008, *A&A*, 478, 111  
 Levinson A., 2000, *Phys. Rev. Letters*, 85, 912  
 Li Y.-R., Yuan Y.-F., Wang J.-M., Wang J.-C., Zhang S., 2009, *ApJ*, 699, 513  
 Lyubarsky Y. E., 2005, *MNRAS*, 358, 113  
 Lyutikov M., 2006a, *New Journal of Physics*, 8, 119  
 Lyutikov M., 2006b, *MNRAS*, 369, L5  
 Lyutikov M., Uzdensky D., 2003, *ApJ*, 589, 893  
 Macchetto F., Marconi A., Axon D. J., Capetti A., Sparks W., Crane, P., 1997, *ApJ*, 489, 579  
 Mahmud M., Gabuzda D. C., Bezrukovs V., 2009, *MNRAS*, 400, 2  
 McKinney J. C., Blandford R. D., 2009, *MNRAS*, 394, L126  
 Moll R., 2009, *A&A*, 507, 1203  
 Moll R., Spruit H. C., Obergaulinger M. 2008, *A&A*, 492, 621  
 Narayan R., Kumar P., 2008, *MNRAS*, 394, L11  
 Neronov A., Aharonian F. A., 2007, *ApJ*, 671, 85



- Owen F. N., Eilek J. A., Kassim N. E., 2000, *ApJ*, 543, 611  
Perlman E. S., Sparks W. B., Radomski J., Packham C., Fisher R. S., Piña R., Biretta J. A., 2001, *ApJ*, 561, L51  
Petschek H. E., 1964, in NESS W.N., e.d., NASA SP-50, The Physics of Solar Flares. NASA Science and Technical Information Division, Washington DC, p. 425  
Piner B. G., Edwards P. G., 2004, *ApJ*, 600, 115  
Reynolds, C. S., Fabian A. C., Celotti A., Rees M. J., 1996, *MNRAS*, 283, 873  
Sikora M., Begelman M. C., Rees M. J., 1994, *ApJ*, 421, 153  
Sparks W. B., Biretta J. A., Macchetto F., 1996, *ApJ*, 473, 254  
Spencer R. E., Junor W., 1986, *Nature*, 321, 753  
Sreekumar P., et al., 1996, *ApJ*, 464, 628  
Stawarz Ł., Aharonian F., Kataoka J., Ostrowski M., Siemiginowska A., Sikora, M., 2006, *MNRAS*, 370, 981  
Tavecchio F., Maraschi L., Ghisellini G., 1998, *ApJ*, 509, 608  
Tavecchio F., Ghisellini G., 2008, *MNRAS*, 385, L98  
Watanabe N., Yokoyama T., 2006, *ApJ*, 647, L123  
Whysong D., Antonucci R., 2004, *ApJ*, 602, 116  
Zenitani S., Hesse M., Klimas A., 2009, *ApJ*, 696, 1385